Journal Pre-proofs

Development of photocatalytic paint based on TiO_2 and photopolymer resin for the degradation of organic pollutants in water

Md.T. Islam, Arieana Dominguez, Reagan S. Turley, Hoejin Kim, Kazi A. Sultana, MAI Shuvo, Bonifacio Alverado-Tenerio, Milka O. Montes, Yirong Lin, Jorge Gardea-Torresdey, Juan C. Noveron

PII: S0048-9697(19)35399-9
DOI: https://doi.org/10.1016/j.scitotenv.2019.135406
Reference: STOTEN 135406

To appear in: *Science of the Total Environment*

Received Date: 31 July 2019
Revised Date: 5 November 2019
Accepted Date: 5 November 2019

Please cite this article as: Md.T. Islam, A. Dominguez, R.S. Turley, H. Kim, K.A. Sultana, M. Shuvo, B. Alverado-Tenerio, M.O. Montes, Y. Lin, J. Gardea-Torresdey, J.C. Noveron, Development of photocatalytic paint based on TiO_2 and photopolymer resin for the degradation of organic pollutants in water, *Science of the Total Environment* (2019), doi: https://doi.org/10.1016/j.scitotenv.2019.135406

Development of photocatalytic paint based on TiO_2 and photopolymer resin for the degradation of organic pollutants in water

Md. T. Islam,[abc] Arieana Dominguez,[a] Reagan S. Turley,[a,c] Hoejin Kim,[e] Kazi A. Sultana,[d] MAI Shuvo,[e] Bonifacio Alverado-Tenerio,[f] Milka O. Montes,[b] Yirong Lin,[e] Jorge Gardea-Torresdey,[a,c,d] Juan C. Noveron [ac*]*

[a] Department of Chemistry, University of Texas at El Paso, 500 West University Avenue, El Paso, TX 79968, USA

[b] Department of Chemistry, University of Texas Permian Basin, 4901 E University Blvd, Odessa, TX 7976

[c] NSF Nanosystems Engineering Research Center for Nanotechnology Enabled Water Treatment (NEWT), Rice University, MS 6398, 6100 Main Street, Houston, USA

[d] Department of Environmental Science and Engineering, University of Texas at El Paso, 500 West University Avenue, El Paso, TX 79968, USA

[e] Department of Mechanical Engineering, University of Texas at El Paso, 500 West University Avenue, El Paso, TX 79968, USA

Instituto de Ciencias Biomédicas, Universidad Autónoma de Ciudad Juárez, Av. Plutarco Elías Calles # 1210, Fracc.Foviste Chamizal Ciudad Juárez, Chih., México. C.P 32310

Graphical Abstract

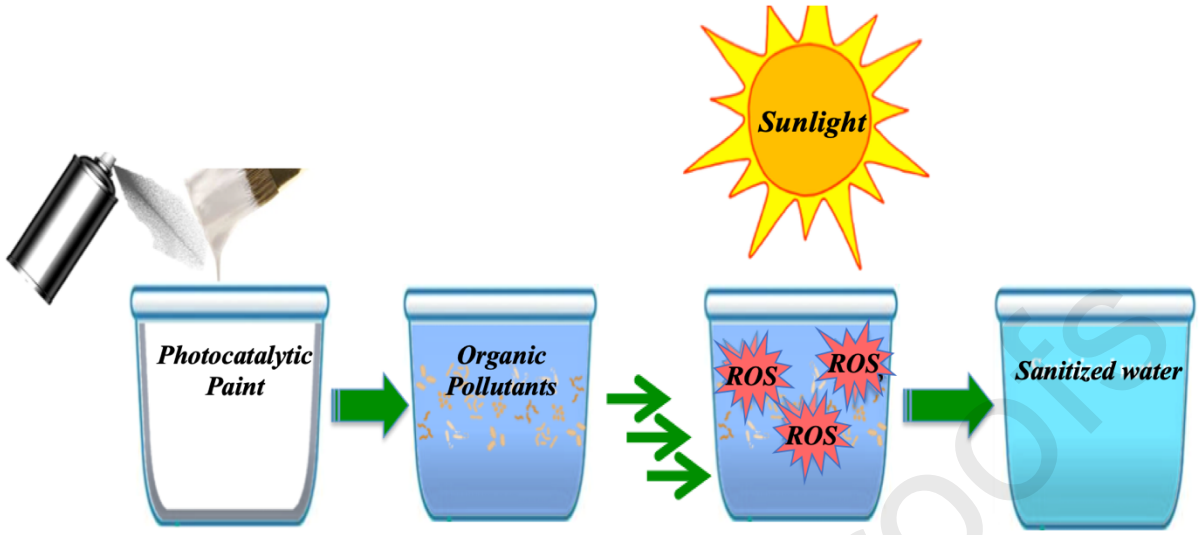

Development of photocatalytic paint based on TiO_2 nanoparticles and photopolymer resin for the degradation of organic pollutants in water under ultraviolet and sunlight irradiation.

Highlights:

- Development of photocatalytic paint based on TiO_2 and photopolymer resin.
- Applicability of the paint on various solid substrates.
- Photocatalytic activity of the paint to degrade organic pollutants.
- Efficient degradation of organic pollutants with high cyclic stability.
- Generation of hydroxyl radicals under sunlight irradiation.

Key Words: Photocatalytic paint, Titanium dioxide (TiO_2), Photopolymer resin, TiO_2 immobilization, Photocatalysis, Water treatment.

Abstract

While the use of TiO2 nanoparticles in the form of slurry/suspension requires energy-intensive separation processes, its immobilization in solid support may open new opportunities in the area of sustainable water treatment technologies. In this study, a novel method for the development of photocatalytic paint based on TiO_2 nanoparticles and acrylate-based photopolymer resin is reported. The paint (TiO_2@polymer) was applied on substrates such as plastic petri dish and glass jar, which was polymerized/solidified by ultraviolet light irradiation. The painted petri dish and glass jar were used for the photocatalytic degradation of model organic pollutants *viz.* methyl orange (MO), methylene blue (MB), and indole in deionized water, simulated fresh drinking water, and tap water matrices. The photocatalytic degradation studies were performed under sunlight and UV-B light were used for. The sunlight-assisted

photocatalytic degradation of MO and MB was found to be faster and more efficient than the UV-B light-assisted ones. Under UV-B light irradiation, it took 120 min to degrade about 80 % of 6 ppm MB solution, whereas under sunlight irradiation it took 60 min to degrade about 90 % of the same MB solution. The photocatalytic paint generated hydroxyl radical (•OH) under the UV-B and sunlight irradiation, which was studied by the terephthalic acid fluorescence tests. Further, the potential release of TiO_2 during the exposure to UV irradiation was studied by single particle ICP-MS analysis.

1. Introduction

Photocatalytic processes are gaining much attention towards the degradation of hazardous pollutants in water.[1] Because of the nature of sustainability, requirements of no chemicals, and generation of no secondary pollutants photocatalytic processes are gaining such attention.[2] While other methods (adsorption, precipitation, coagulation-flocculation, ion-exchange, etc.) mostly transfer pollutants from one phase to another, photocatalytic processes degrade them to mineralization.[2] Under sunlight or UV light irradiation, photocatalysts produce highly oxidative reactive oxygen species (radicals) that can destroy organic pollutants to CO_2 and H_2O, which is also known as mineralization. In addition, photocatalysts are also widely studied for the preparation of self-disinfecting surfaces, degradation of the indoor and outdoor volatile organic pollutants (VOCs and NOx) and odors in the air, and in the development of self-cleaning textiles.[3,4,5]

Among various photocatalysts, titanium dioxide (TiO_2) is the most extensively studied and employed one.[6,7,8,9] Under the ultraviolet (UV) light illumination, TiO_2 demonstrates an extraordinary ability towards the degradation of organic pollutants through the redox-reactions driven by the excited electrons and holes between the valence and conduction bands.[10]

Additionally, its ability to generate reactive oxygen species (ROS)/oxidative radicals makes it an excellent candidate for the photocatalytic disinfection of water.[11,12]

The conventional method for the use of TiO_2 involves the slurry-suspension, where the TiO_2 nanoparticles powder is dispersed in contaminated water in the form of a slurry or suspension.[13,14] Although the TiO_2 particles in the form of slurry can utilize the maximum light absorption and mass transfer of pollutants, the method suffers from some major drawbacks. For example, the particles need continuous mixing during photocatalysis process to keep them suspended. After the photocatalysis, the TiO_2 nanoparticles require complete and effective separation from the reaction mixture for the sake of environmental safety and sustainability. The post-photocatalysis separation of the TiO_2 particles usually requires difficult and high-energy consuming processes such as ultrafiltration, ultracentrifugation, and effective precipitation. Because of these drawbacks of slurry suspension method, photocatalytic water treatment processes are not receiving widespread acceptance in practical applications.[15,16,17]

To avoid the drawbacks of the slurry-suspension method, approach such as the immobilization of TiO_2 particles in a solid matrix has become an intriguing alternative.[18,19,20] The immobilization of TiO_2 particles avoids the requirement for the energy-intensive separation of the catalyst and at the same time facilitates the recycling and reusability of the catalyst. For example, TiO_2 has been reported to be immobilized in cement,[21] different types of polymers,[22,23,] paints,[24,25,11,12] cellulose,[26] glass,[27] ceramics,[28] silica gel,[29] clays,[30] graphene,[31] carbon nanotubes,[32] and others. Audrey Bonnefond and colleagues reported the preparation of stable photocatalytic paints based on acrylic polymer and TiO_2 nanoparticles for bacterial inactivation.[11,12] Koichi Kobayakawa and colleagues reported the immobilization of TiO_2 nanoparticles on the silica gel beads of 2 mm diameter followed by the utilization in a

continuous-flow photoreactor for the degradation of oxalic acid as the model contaminant.[17] Mohammad Delnavaz and colleagues reported the application of concrete surfaces as the substrate for immobilization of TiO_2 nanoparticles in the photocatalytic treatment of phenolic water.[12] Other techniques, such as agglomeration of the TiO_2 nanoparticles to facilitate the easy recovery, has also been reported.[33] For instance, Padro Alvarez and colleagues used micrometer-sized TiO_2 hierarchical spheres decorated with cyclodextrin that self-precipitate quickly from the suspension for the degradation of organic micropollutants in water.[21] Most of these methods are limited to a particular type of substrate/matrices, need sophisticated procedure, instrumentations, hazardous chemicals, and may suffer from scalability and industrial adaptability. The goal of this study was to develop a novel photocatalytic paint employing a facile method and to study its photocatalytic activity towards the degradation of model organic pollutants in water. Although the development of some photocatalytic paints has been reported before, the preparation of photocatalytic paint based on commercially available photopolymer resin and TiO_2 has not been reported, to the best of our knowledge. This study is unique in terms of the simplicity of the preparation of the paint. The paint can be prepared just by mixing the photopolymer resin with TiO_2. The method does not require any sophisticated technique and hazardous solvents/chemicals. Moreover, the method has adaptability to large-scale preparation and applicability to numerous solid substrates. Moreover, the application of the paints in the degradation of aqueous organic pollutants under sunlight and UV light irradiation has not been thoroughly studied in the literature, to the best of our knowledge. Therefore, a facile method for the development of photocatalytic paint as well as its application in the degradation of various organic pollutants can lead towards a sustainable water treatment technology. The photocatalytic paint may play an important role in paving the way to the development of photoactive coatings

and 3-D polymer blends capable of accelerating innovations in practical and sustainable environmental remediation technologies.

In this study, a very simple, novel, and hazardous chemicals-free method for the development of photocatalytic paint consisting of TiO_2 nanoparticles and acrylate-based photopolymer resin is presented. The TiO_2 nanoparticles were dispersed in the acrylate photopolymer resin and applied as a paint on solid substrates such as plastic petri dish and glass jar. Later, the paint was polymerized/solidified on the substrates by UV-light irradiation. The polymerization/solidification of the photopolymer resin caused the immobilization of the TiO_2 nanoparticles by physical non-bonding interactions. The painted petri dish and glass jar were used for photocatalytic degradation of organic pollutants *viz.* methyl orange (MO), methylene blue (MB), and indole in deionized water, simulated fresh drinking water, and tap water matrices under the sunlight and UV-B light irradiation. Methyl orange, methylene blue, and indole were used as the model pollutants because they are known to be toxic, carcinogenic, and mutagenic to the environment.[34,35,36]

2. Materials and Methods

2.1. Materials

TiO_2 -P25 nanopowder (≥99.5 % trace metals basis, 21 nm by TEM), sodium hydroxide (NaOH ≥ 98 %), and Terephthalic acid [C8H6O4 = 98 % were obtained from Sigma Aldrich. Clear Plastic Sterile Petri Dishes of 60 mm x 15 mm dimensions was purchased from Shxstore. Acrylate-based photopolymer resin (Clear Resin RS-F2-GPCL-04) was obtained from Formlabs. Methylene blue and methyl Orange ($C_{14}H_{15}N_3O_3S$ >98.0 %) were purchased from EMD Millipore Corporation and TCI AMERICA, respectively. UVP Ultraviolet Crosslinker (Model CL-1000) having UV-B fluorescent tube lamps, was used as the source of UV light of about 302

nm wavelength, as per the specification of the vendor. Digital Light Meter LX1330B was used to measure the light intensity and it was about 21,5000 lux on the surface of the petri dish. Milli-Q (Advantage A-10) water filter system supplied the Milli-Q water (> 18.20 MI cm resistivity), which is referred to as deionized water (DIW). Simulated fresh drinking water, denoted as FDW, was prepared by dissolving various salts viz. $CaCl_2.2H_2O$ (147 mg), $NaHCO_3$ (252 mg), $Na_2SiO_3.9H_2O$ (95 mg), $MgSO_4.7H_2O$ (124 mg), $NaNO_3$ (12 mg), $NaH_2PO_4.H_2O$ (0.18 mg), and, NaF (2.2 mg) in 1 L of DIW. Tap water was obtained from the laboratory faucet. The approximate composition of the tap water is given in supporting information, Figure S1.

The potential release of TiO_2 during the exposure to UV irradiation was studied by single particle ICP-MS analysis. Total titanium determination was performed using a Perkin Elmer NexION 1000 ICP Mass Spectrometer. Titanium was measured using the ^{49}Ti isotope to avoid polyatomic interferences for the most prevalent isotope of titanium, ^{48}Ti. The sample flow rate of the nebulizer was 0.263 mL/min with a transport efficiency of 6.19% using nanoComposix gold spheres (60 nm NanoXact Citrate coated Gold Nanospheres) as a particle standard. Data acquisition and analysis was performed using the Nano Application Module in the Syngistix software suite. An acquisition time of 120 seconds per measurement was used including a dwell time of 100 μs.

2.2. Preparation of the photocatalytic paint/ TiO_2@polymer

Photocatalytic paint (consisting of a mixture of TiO_2 and photopolymer resin) having different weight percentage of TiO_2 (0-10 wt. %) was prepared in plastic petri dishes. Required amount of TiO_2 nanoparticles and photopolymer resin were weighed out in the petri dish and thoroughly mixed with a spatula followed by bath sonication for 10 min. In every petri dish, an overall weight of the TiO_2 nanoparticles and photopolymer resin was 1 g. Later, the mixture was

polymerized in the ultraviolet box reactor for 30 min to 4 hours to obtain a solid/polymerized mass (TiO_2@polymer). For instance, to obtain 10 wt. % TiO_2@polymer, 100 mg TiO_2 nanoparticles were thoroughly mixed with 900 mg of the photopolymer resin in the petri dish. The mixture was then photopolymerized in the ultraviolet box reactor for about 4 h to obtain a solid/polymerized mass. Following the same procedure, five petri dishes were prepared having 0, 1, 2.5, 5, and 10 wt. % of TiO_2.

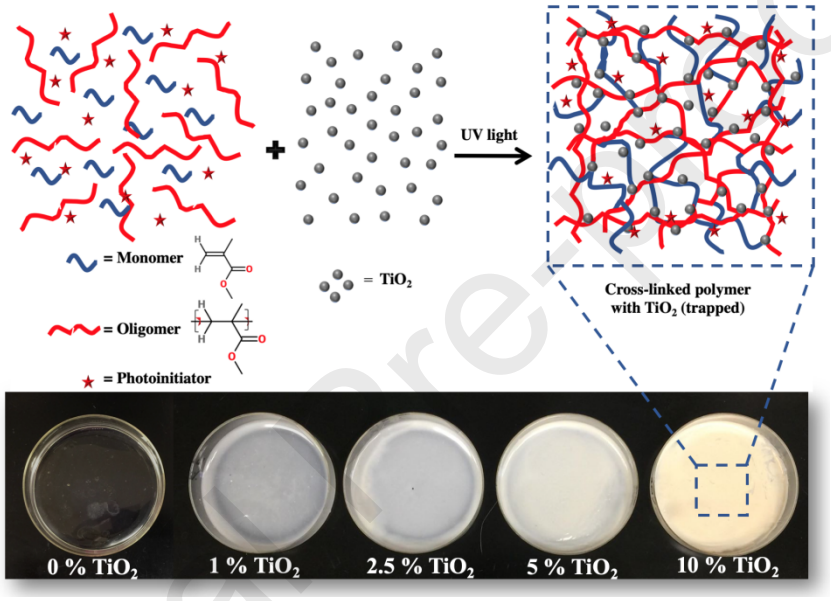

Scheme 1. Scheme showing the preparation of the TiO_2@polymer. Plastic petri dishes showing the TiO_2@polymer with varying weight percentage of TiO_2.

It was observed that the time for the complete polymerization/solidification of the TiO_2@polymer resin varied from 30 min to 4 hours. Pure resin took about 30 min to completely polymerize/solidify; however, the TiO_2@polymer resin took longer time with the increase in the weight percentage of TiO_2. Due to the presence of TiO_2, the UV light penetration through the resin was retarded and thereby it took longer time to polymerize/solidify. The immobilization of TiO_2 in the photopolymer resin through UV light induced polymerization could be schematically represented by Scheme 1.

2.3. Characterization techniques

Various characterization techniques such as Transmission electron microscopy (TEM), Scanning electron microscopy (SEM), Energy dispersive X-ray spectroscopy (EDX), UV-visible spectroscopy, X-ray powder diffraction (XRPD), and X-ray photoelectron spectroscopy (XPS) were utilized to characterize the TiO_2@polymr. For example, TEM and SEM revealed the morphology of the TiO_2 and their successful immobilization to the polymer matrix. The X-ray powder diffraction analysis demonstrated the crystalline properties of the TiO_2@polymer, whereas the solid-state UV visible spectroscopy was used to determine the bandgap of the TiO_2 nanoparticles. Agilent Cary 50 Conc UV-Visible Spectrophotometer having quartz cuvette of 10 mm path length was for the UV-visible spectroscopic studies of MO and MB solution. Solid-state UV-Vis spectrum of TiO_2 was obtained by using Cary 5000 UV-Vis-NIR having a stainless-steel sample holder. High-resolution TEM (HRTEM) and typical TEM images were obtained by using JEOL JEM3200FS and Hitachi H-7650 Microscope, respectively. 300 kV and 80 kV acceleration voltage were used for the JEOL JEM3200FS and Hitachi H-7650 Microscope, respectively. Carbon filmed copper grid with 200 mesh (Electron microscopy sciences) was drop-casted and dried with a suspension of TiO_2 nanoparticles in ethanol for the imaging analysis. SEM images and EDX spectrum were obtained by using a JEOL JSM-IT100 scanning electron microscope (SEM) equipped with EDX facility. SEM Pin Mount Specimen Holders was used as the substrate for the SEM imaging. Powder X-ray diffraction (XRPD) pattern collected by using Bruker D8 Discover X-ray diffractometer equipped with Cu Kα radiation ($\lambda = 0.15418$ nm).

2.4. Methyl Orange and Methylene blue Degradation Experiments

Methyl orange and methylene blue solutions having concentration of 6 ppm (or mg/L) in DIW and simulated FDW were used for the photocatalytic experiments. In the photodegradation experiments, 10 ml of MO or MB solution was poured into the petri dish. The dye solution was illuminated in the UV box reactor and at a regular interval of 20 min about 1 mL dye solution was withdrawn for UV-visible spectroscopic analysis. The dye solution was put back to the petri dish after the UV-visible studies.

For the photocatalytic degradation of MO and MB under sunlight irradiation, the same experimental procedure was employed except the irradiation under the direct sunlight. The average intensity of sunlight was about 100,0000 lux. Under sunlight, it was found the about 2.5 mL of the water evaporated out during 60 min of irradiation. Therefore, the percent degradation was normalized with respect to the volume change (only for MO) during the photocatalysis.

For recyclability experiments, petri dish having 10 wt. % TiO_2 was used for the degradation of MB solution. Five cycles of photocatalysis was carried out over a period of one month to evaluate the stability and cyclic stability of the TiO_2@polymer.

To study the release of TiO_2 under UV irradiation, 10 mL water was irradiated for 60 min in the plastic petri dishes having 10 and 5 % TiO_2. The UV irradiated water was later analyzed by the single particle ICP-MS.

2.5. Terephthalic acid Fluorescence Test for the Measurement of •OH

For the terephthalic acid fluorescence test, 10 ml of 5 $\times 10^{-3}$ M sodium terephthalate solution was irradiated with light (UV and sunlight) in the petri dishes having TiO_2@polymer. About 0.8 mL of the solution was withdrawn at every 20 min interval of time for the fluorescence study. Aqueous solution of sodium terephthalate was prepared by reacting terephthalic acid with stoichiometric amount of NaOH in deionized water.

3. Results and Discussion

Titanium dioxide (TiO_2) is one of the most active photocatalysts for the efficient degradation of organic pollutants in water. However, its use in the form of slurry suspension limits its potential practical application due to the requirement of energy intensive and expensive separation processes of the nanoparticles. Therefore, the immobilization of the TiO_2 nanoparticles on a solid substrate is gaining much attention as an intriguing alternative to the slurry suspension method. This in turn may facilitate its practical applications for the sustainable water treatment technologies. Herein, TiO_2 nanoparticles were dispersed in acrylate-based photopolymer resin to obtain a paint-like substance. The paint-like substance was applied on solid substrates such as plastic petri dish and glass jar. The paint was solidified on the substrates by UV light-induced polymerization of the photopolymer resin. The resin consists of acrylate-based monomer, oligomers, and photo initiators. The polymerization of the resin trapped and immobilized the TiO_2 nanoparticles throughout the polymer matrix. The solidified paint having immobilized TiO_2 was thoroughly characterized and utilized for the photocatalytic degradation of hazardous organic pollutants (MO, MB, and indole) using UV and sunlight irradiation.

3.1. SEM Images and EDS Spectrum of the TiO_2@polymer

While the surface morphology of the TiO_2@polymer was analyzed by the SEM image analysis, the elemental composition was investigated by the SEM-EDX analysis. The SEM images of the just polymer and the TiO_2@polymer (10 wt. % TiO_2) are shown in Figure 1a and 1b, respectively. As shown in Figure 1a, just polymer surface was seen smooth without having any particles or aggregations on it. On the other hand, the TiO_2@polymer surface could be seen as rough having TiO_2 nanoparticles in the form of small aggregation. This indicated the immobilization or attachment of TiO_2 nanoparticles in the form of aggregation on the surface of

the polymer.

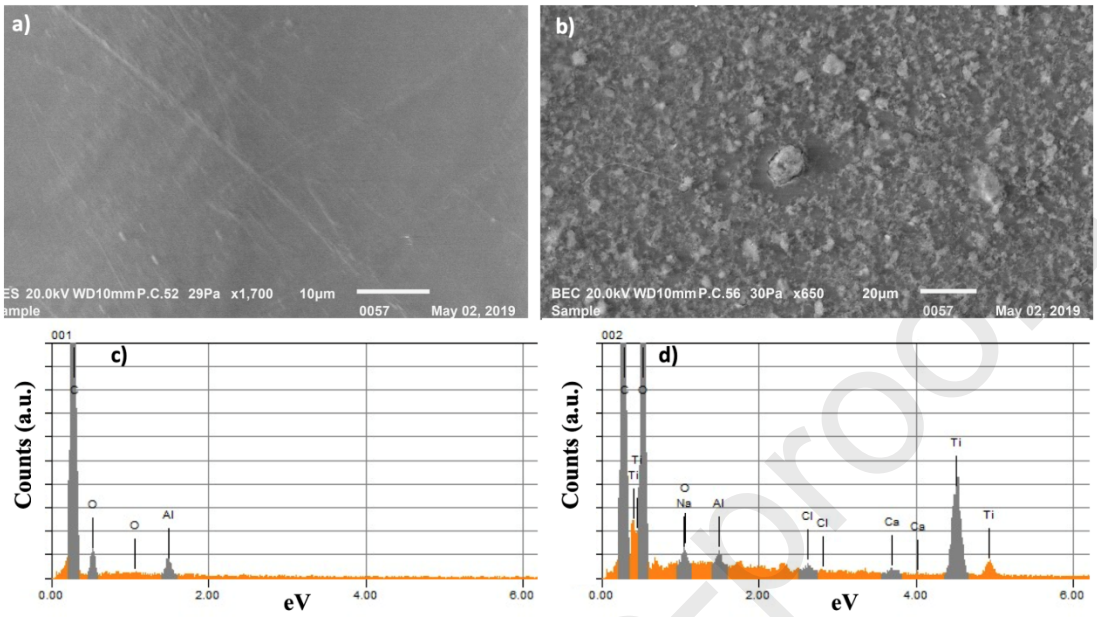

Figure 1. Typical SEM images of the a) just polymer and b) TiO_2@polymer having 10 wt. % TiO_2. The EDX spectrum of the c) just polymer and d) TiO_2@polymer having 10 wt. % TiO_2.

The EDX spectrum of the just polymer showed the presence of carbon and oxygen, which indicated the constituting elements of the acrylate polymer, Figure 1c. On the other hand, the EDX spectrum of the TiO_2@polymer showed a high abundance of Titanium in addition to Carbon and Oxygen, Figure 1d. The presence Titanium further suggested the presence and eventually the successful immobilization of the TiO_2 nanoparticles in the polymer matrix. The aluminum peak at the EDX spectrum originated from the aluminum substrate that was used as the sample holder for the analysis.

3.2. TEM and HRTEM images of TiO_2 Nanoparticles

Typical and high-resolution TEM images of the TiO_2 nanoparticles are shown in figure 2a and 2b, respectively. The TiO_2 nanoparticles were seen with a variety of shapes having predominantly spherical. The TiO_2 nanoparticles were found somewhat faceted and the average

diameter of the nanoparticles were calculated to be about 21 nm, which is as specified by the vendors. The HRTEM image shows the crystalline lattice spacings of the TiO_2 nanoparticles, Figure 2b. The d-spacing measurement of 2.33 Å corresponds to the (112) planes of the TiO_2 nanoparticles.

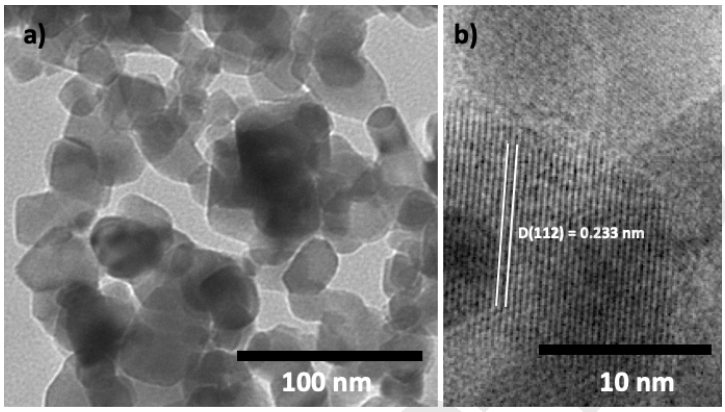

Figure 2. a) Typical and b) high-resolution TEM images of the TiO_2 nanoparticles.

3.3. Solid state UV-Visible spectroscopy, XPS, and XRPD pattern of the TiO_2 Nanoparticles

Solid-state UV-visible diffuse reflectance spectrum (DRS) of the TiO_2 nanoparticles is shown in Figure 3a. The TiO_2 nanoparticles showed a significant absorption of light below 400 nm, which indicated the strong UV light absorption ability of the TiO_2 nanoparticles. The absorption cutoff was found to be 395 nm and bandgap was calculated to be 3.15 eV using the equation E=hv, where E is the energy of photon in eV, h is Planck's constant ($6.62607004 \times 10^{-34}$ m^2kg/s), and v is the frequency of the absorption cutoff (shown by the green arrow in Figure 3a).

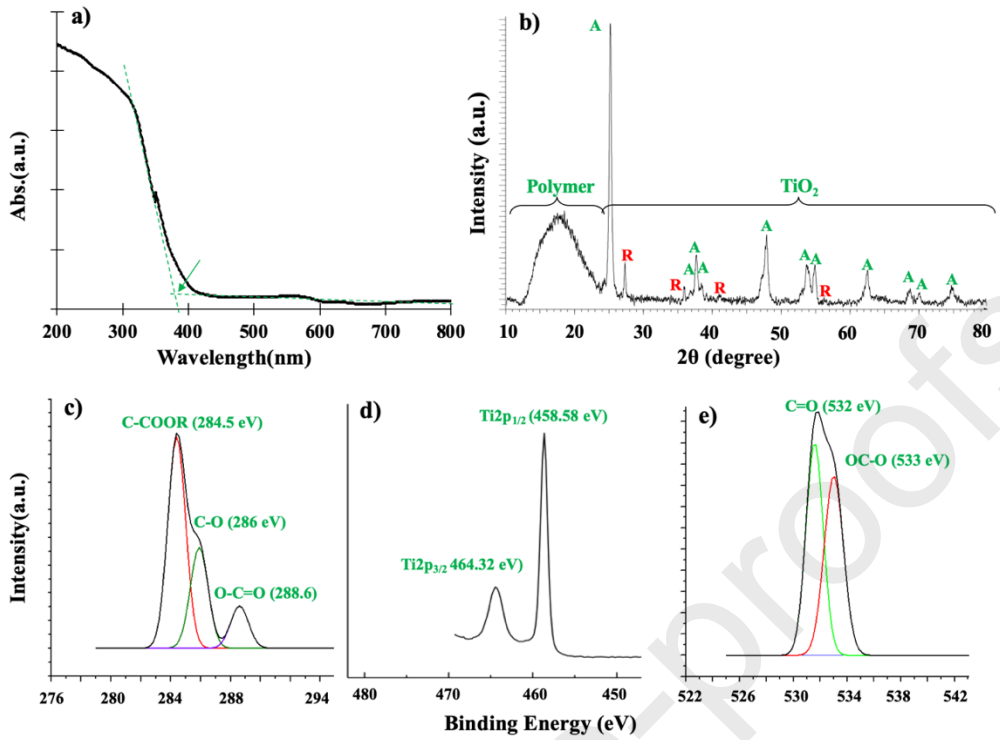

Figure 3. a) UV-Visible DRS spectrum of TiO_2 nanoparticles, b) XRPD patterns of TiO_2@polymer showing amorphous polymer, anatase (A), and rutile (R) crystalline phases, c) High-resolution XPS spectra of C1s, d) Ti2p, and e) O1s.

X-ray powder diffraction (XRPD) analysis was performed to study the crystalline structures of the TiO_2@ polymer, Figure 3b. Based on the XRPD pattern, the TiO_2 nanoparticles were found to be highly crystalline. The characteristic diffraction peaks at 2θ = 25.3°, 36.9°, 37.7° 38.6°, 47.9°, 53.8°, 55°, 62.6°,68.8°, 70°, and 74.9° can be assigned to the (101), (103), (004), (112), (200), (105), (211), (204), (116), (220) and (215) planes of anatase TiO_2 (JCPDS No. 71-1166), respectively.[37,38] However, the peaks at 2θ = 27.3°, 36°, 41.1°, 55.1°, and 56.2°, can be assigned to the (110), (101), (111), (211), and (220) planes of rutile TiO_2 (JCPDS No. 73-1763), respectively.[35] Therefore, the XRPD pattern indicated that the TiO_2 nanoparticles was composed of both Anatase and Rutile crystalline forms, which is in compliance with the vendor's specification. The TiO_2 (P25) composed of 80 % anatase and 20 % rutile crystalline

phases as per the vendor specification.[39] In addition to the characteristic peaks for TiO_2, a broad peak was found at 2θ = 18°, which indicated the amorphous nature of the polymer in TiO_2@polymer.

The chemical composition of the TiO2@polymer (10 % wt.) was further investigated via high-resolution XPS (HRXPS) of C 1s, Ti 2p and O 1s, Figure 3c-e. The C 1s peaks at ~284.5 eV, ~286 eV, and 288.6 eV could be identified as C–COOR, C-O, and O-C=O bonds of the polymer, respectively (Figure 3c).[40,41] Additionally, two O 1s peaks at 532 eV and 533 eV could be identified as C=O and OC-O of the polymer, respectively (Figure 3e).[37,38] For TiO_2, the signal over noise ratio of Ti 2P peaks, obtained from the TiO2@polymer, was very week. Therefore, the Ti 2p XPS peaks were obtained by using pure and dried TiO_2 powder. The Ti 2p peaks at 558.6 eV and 464.3 eV could be identified as the Ti 2p1/2 and Ti 2p3/2 binding energies of TiO_2 nanoparticles (Figure 3c).[42] The surface atomic percentage of elements were found to 75.97 % C, 23.6 % O, and 0.43 % Ti, which indicted that most of the TiO_2 nanoparticles settled down on the bottom of the petri dish during the time of photopolymerization.

3.4. Photocatalytic Degradation of Methyl Orange and Methylene Blue

The photocatalytic activity of the TiO_2@polymer was studied by the degradation of methyl orange (MO) and methylene blue (MB) in two different types of water matrices. The degradation of these dyes was monitored by the decrease in their characteristic absorption bands (for MO at 463 nm and for MB at 665 nm).[43,44,45,46]

The percentage degradation of the pollutants was calculated using the following equation.

$$Percentage\ Degradation = \frac{C - Ct}{Co} \times 100\ \% = \frac{Ao - At}{Ao} \times 100\ \%$$

where, C_o, and Ct represents the initial and time-dependent concentration of MO and MB; A_o

and A_t represent the initial and time-dependent absorbance of MO and MB.

The photocatalytic performance of the TiO_2@polymer towards the degradation of MO (6 ppm) and MB (6 ppm) in DIW under UV light irradiation is demonstrated in Figure 4. As of Figure 4a, it was found that the polymer matrix having (1-10 wt. % TiO_2) degraded more than 90 % MO after 120 min of light irradiation. On the other hand, the bare polymer removed about 10 % MO after 120 min while just MO solution showed about 3 % MO decolorization. Polymer matrix having more TiO_2 showed faster activity; however, the activity was not linear with respect to the percent weight of TiO_2 loading in the polymer matrix.

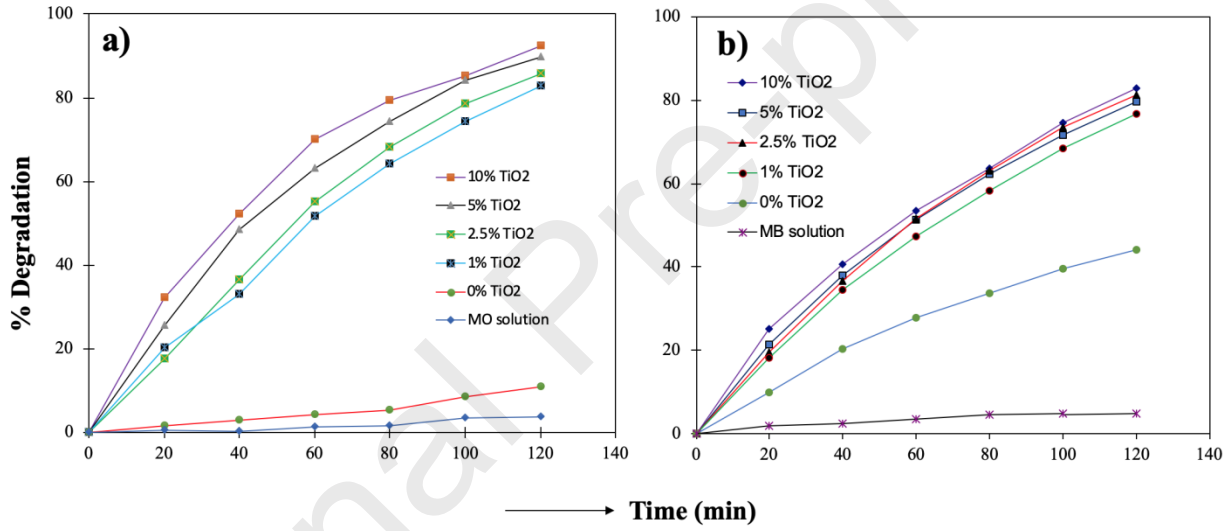

Figure 4. Photocatalytic degradation of a) MO and b) MB in DIW under UV light irradiation.

Likewise, the TiO_2@polymer demonstrated enhanced performance in the degradation of MB, Figure 4b. About 80 % MB was decolorized after 120 min of UV light irradiation. Interestingly, it was found that just polymer also showed about 40 % decolorization of the solution after 120 min. The origin of the photocatalytic activity of the bare polymer is further studied by its ability to generate hydroxyl radical in water, which is discussed in section 3.7.

The photocatalytic performance of the TiO_2@polymer was further studied by the degradation of MO, MB, and indole in aqueous solution under sunlight irradiation, Figure 5 and

6. Indole solution was used to check the photoactivity of the TiO_2@polymer in the degradation of colorless transparent compound. The degradation of MB and MO was performed in two different water matrices (DIW and simulated FDW), while indole degradation was carried out in DIW. The degradation of the pollutants under sunlight irradiation caused the loss of about 2.5 mL of water by evaporation (after 80 min.) and thereby the percentage degradation of MO was normalized with respect to the volume change. For the degradation of MB and indole, the percentage degradation was not normalized as it was found their degradation was faster than MO. Figure 5a and 5b shows the degradation of MO solution in simulated FDW and DIW matrices, respectively. It was found that the TiO_2@polymer degraded 40-80 % MO in the DIW after 80 min of sunlight irradiation, whereas 60-95 % MO degradation was observed in the simulated FDW matrix. This study indicated that the TiO_2@polymer was even more active in degrading MO in the presence of dissolved ions in water.

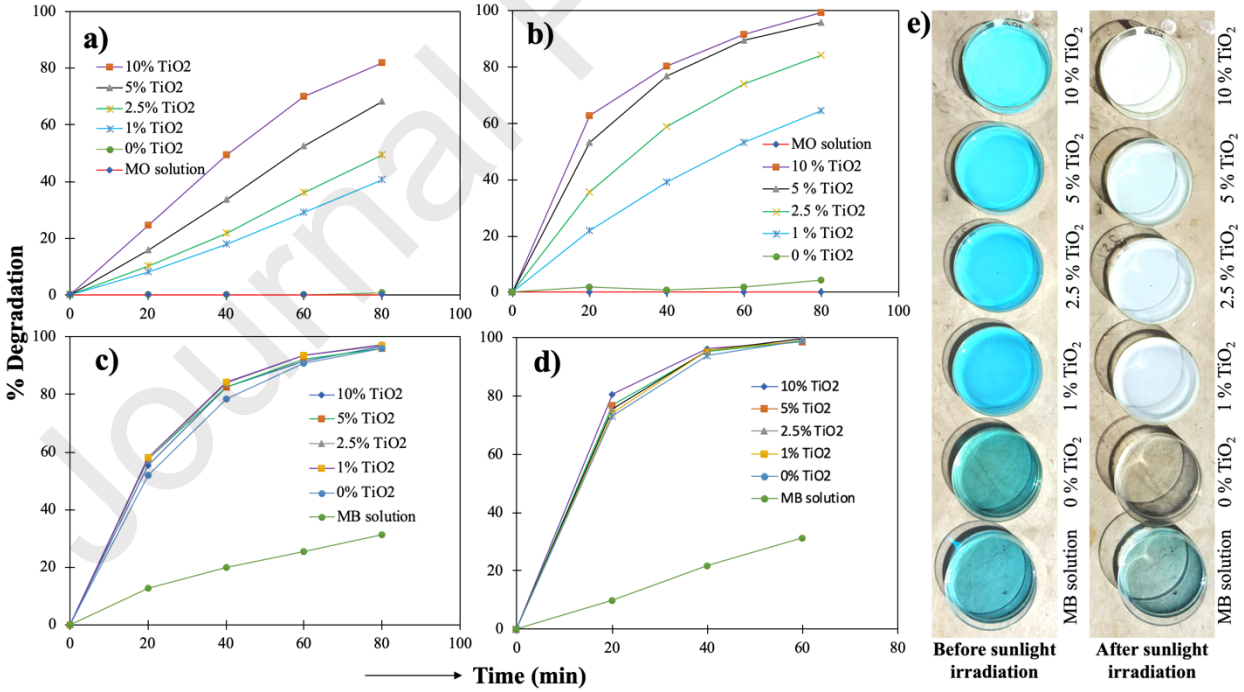

Figure 5. Photocatalytic degradation of MO and MB under sunlight irradiation. a) MO solution

in DIW, b) MO solution in simulated FDW, c) MB solution in DIW, d) MB solution in simulated FDW, and e) digital image for the photocatalytic degradation of MB in simulated FDW under sunlight irradiation.

Similar results were obtained in the degradation of MB under the sunlight irradiation, Figure 5c and 5d. Almost complete decolorization of MB solution was observed after 80 and 60 minutes of irradiation in DIW and simulated FDW matrices, respectively. Moreover, the degradation of MB in simulated FDW matrix was found to be faster compared to the DIW matrix, which is similar to the MO degradation. Also, the MB degradation was found to be faster compared to MO, which could be attributed to the self-degradation of just MB solution under the sunlight irradiation, Figure 5c and 5d. About 30 % of the MB solution was found to self-degrade just by sunlight irradiation. Interestingly, the petri dish having no TiO_2 showed almost equal activity as of those having TiO_2 nanoparticles. The origin of the photocatalytic activity of the pure polymer is explained in section 3.7. The digital photograph of the photocatalytic degradation of MB in simulated fresh drinking water under sunlight irradiation is shown in Figure 5e. The petri dish having 10 % TiO_2 demonstrated complete degradation of the MB after 60 min of sunlight irradiation, while the MB solution undergone about 30 % degradation by photobleaching.

The non-linear photocatalytic activity of TiO_2@polymer (with respect to the wt. % of TiO_2 loading) can be explained as follows. Firstly, it was found that the mixture of TiO_2 nanoparticles and photopolymer resin having more wt. % of TiO_2 took longer time to solidify/polymerize. During this time, it was observed that some of the TiO_2 nanoparticles settled down on the bottom of the petri dish. Therefore, although the 10 % TiO_2@polymer had an overall higher wt. % of TiO_2 loading, the amount of TiO_2 on the surface of the petri dish was not

much higher than the one having less TiO_2 loading. Secondly, it could also be because of the aggregation and agglomeration of the TiO_2 nanoparticles on the surface of the polymer (as seen by SEM image), which may have caused the lowering of the effective surface area and light irradiation on the TiO_2 nanoparticles.

In ability of the TiO_2@polymer in the degradation of colorless compound was studied by the degradation of indole in water.[47] The degradation of 6 ppm indole solution in DIW was performed under sunlight irradiation, Figure 6b. In this case, petri dish having 10 wt. % TiO_2 was used along with the pure polymer and just indole solution as the controls. The degradation of indole was monitored by the lowering of the characteristic absorption band of indole at 280 nm determined by UV-visible spectroscopy. The UV visible spectroscopy and the calibration curve is shown in Figure S2.

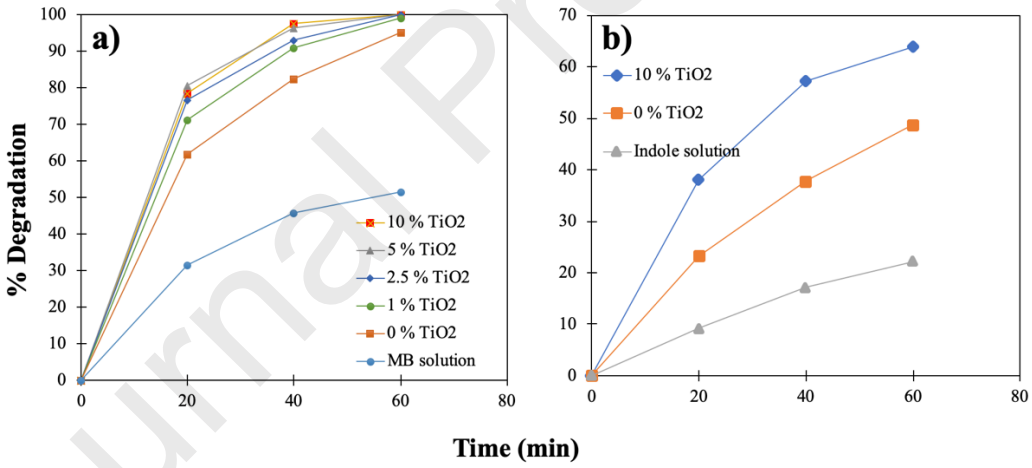

Figure 6. Photocatalytic degradation of a) MB in tap water and b) indole in DIW under sunlight irradiation.

Like MO and MB, the degradation of indole was found to be enhanced by the TiO_2 nanoparticles immobilized in the polymer matrix. It was observed that the petri dish having 10 wt. % TiO_2 degraded about 64 % indole after 60 min of sunlight irradiation; whereas, it was about 49 for petri dish having just polymer. Like other two dyes, it was found that indole

undergone photodegradation just by sunlight irradiation to about 22 %. The photodegradation of MO, MB, and indole in water, without the presence of any catalyst, indicated the presence high percentage of UV light in the sunlight irradiation. Therefore, from the above photodegradation studies it could be concluded that the TiO_2 immobilized in the polymer matrix enhanced the degradation of colorless and colored pollutants in water under sunlight and UV light irradiation.

Finally, the applicability of the photocatalytic paint in the degradation of organic pollutants in real water was studied by the decolorization MB solution in tap water under the sunlight irradiation, Figure 6a. It was observed that the decolorization of MB was enhanced by the immobilization of TiO_2 in the polymer matrix. About 100 % MB was decolorized within 60 min period of sunlight irradiation. This result indicted the applicability of the paint, developed in this study, in the degradation of organic pollutants in real water using sunlight irradiation.

3.5. Recyclability of the paint and the potential of TiO_2 release

Cyclic stability is an important and desirable properties of a photocatalyst. To evaluate the cyclic stability, the TiO_2@polymer having 10 wt. % TiO_2 was employed for 5 cycles of photocatalysis over period of three months, Figure 7.

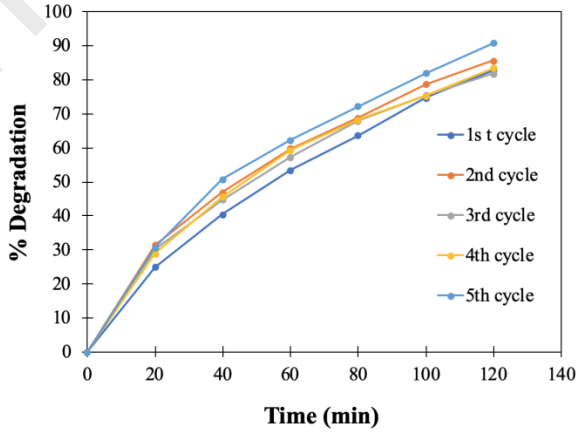

Figure 7. Cyclic stability of the 10 wt. % TiO_2@polymer (10 wt. % TiO_2) for the degradation of 6 ppm MB solution in DIW under UV-light irradiation.

Results revealed that the TiO_2@polymer not only maintained the photocatalytic activity rather it became better with the successive use. We assume that with the successive use the TiO_2 nanoparticles on the surface of the polymer became more exposed and thereby became more accessible to light, solvent, and to the pollutants in solution, which caused the increase in photocatalytic activity.

The calculated particle concentration number was 3.2 x 10^5 particles per mL for the 5% loading and 3.6 x 10^5 particles per mL for the 10% loading petri dishes, respectively. The mean sizes of particles were 95.7 nm in the water from the 5% loading petri dish and 100.1 nm in the 10% loading petri dishes. The most frequent size was 63 nm in both samples. Using the mean size and assuming a spherical shape for the particles, the mass concentration for the two samples was 0.62 ppb for the 5% loading and 0.81 ppb for the water from the 10% loading sample.

3.6. Painted glass jar for the degradation of MB in tap water

In order to demonstrate practical applicability and large-scale adaptability of the paint, a glass jar having volume of about 950 mL was painted with the TiO_2@polymer paint (having 10 % TiO_2) and was utilized for the degradation of MB solution in tap water matrix under sunlight irradiation, Figure 8.

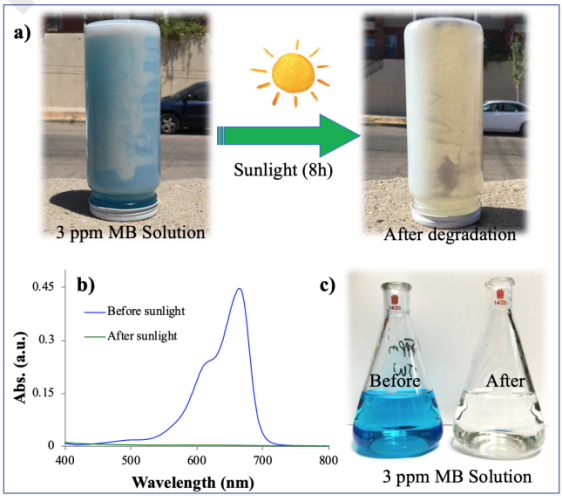

Figure 8. Photocatalytic degradation of 3 ppm MB solution in a painted glass jar under sunlight irradiation.

As shown in figure 8, the painted glass jar degraded 3 ppm MB solution completely after 9 hours of sunlight irradiation. A painted glass jar with MB solution before and after photocatalysis is shown in Figure 8a. The characteristic UV-visible spectrum of the MB solution before and after the photodegradation is shown in Figure 8b, whereas the digital image of the MB solution before and after photodegradation is shown in Figure 8c. Therefore, according to the results of this study it could be suggested that the TiO_2@polymer could be applied as the paint on a solid substrate for the photocatalytic degradation of organic pollutants in water.

3.7. Measurement of •OH generation in the photocatalytic process

The UV-light and sunlight assisted generation of •OH by the TiO_2@polymer was studied by terephthalic acid fluorescence technique. In this technique, terephthalic acid disodium salt is used as the probing molecule. The •OH generated by the photocatalytic processes reacts with terephthalate ion to make fluorescent 2-hydroxyterephthalate that generates blue fluorescence having maximum emission at 425 nm when excited with 315 nm wavelength of light.[48,49] Quantitatively, the fluorescence intensity increases with the increase in the photogeneration of •OH during the photocatalytic reactions.

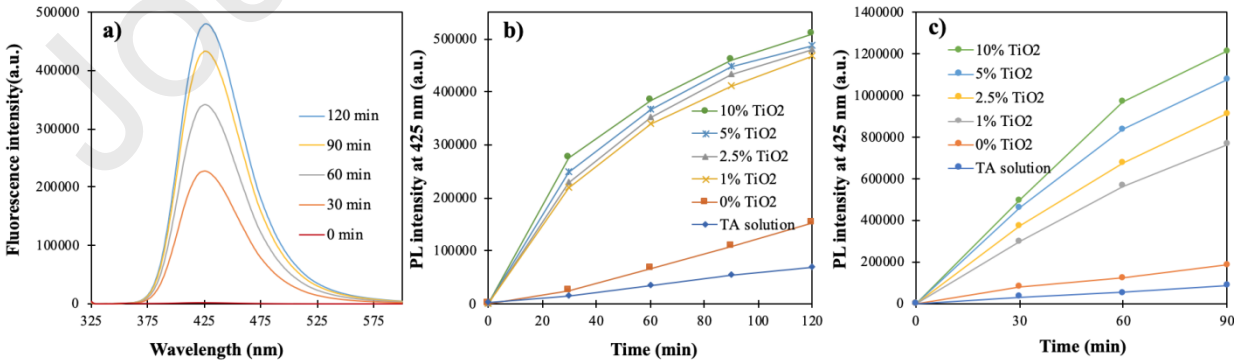

Figure 9. a) Time-dependent fluorescence spectrum of 2-hydroxyterephthalate solution in water

under the irradiation of UV light, b) kinetics of •OH generation by TiO_2@polymer under UV light, and c) kinetics of •OH generation by TiO_2@polymer under sunlight irradiation.

The time-dependent fluorescence emission spectrum of 2-hydroxyterephthalate in water (representative for 10 % TiO_2@polymer) under UV-light irradiation is shown in Figure 9a. The fluorescence intensity increased with the increase in the reaction time, which indicated a gradual increase in the generation of •OH over the time of light irradiation. The kinetics of the photocatalytic generation of •OH under the UV light and sunlight irradiation is shown in Figure 9b and 9c, respectively. It was observed that the TiO_2@polymer generated much more •OH radicals than the bare polymer under both the UV and sunlight irradiation. However, the sunlight generated almost three times more •OH compared to the UV light. This could be attributed to the higher light intensity of the sunlight (100,0000 lux) compared to the UV light (21,5000 lux). Also, it was found that bare polymer and the sodium terephthalate solution generated some amount of •OH under light irradiation. From the vendor's specification, it was found that the photopolymer resin had some fluorescent compounds as the photo initiator, which may have generated the •OH under the light irradiation. This further provides a reason why the pure polymer degraded MB and indole under the sunlight irradiation. From the fluorescence tests it could be concluded that the TiO_2@polymer generated •OH under both the UV and sunlight irradiation. These highly reactive •OH caused oxidative degradation of organic pollutants such as MO, MB, and indole in water.

3.8. Proposed Mechanism of ROS Generation and the Degradation of Organic Pollutants

The mechanism for the generation of ROS followed by the degradation of organic pollutants on the TiO_2 nanoparticles can be proposed as follows, Scheme 2. The mechanism is proposed on the basis of the results of this study and the previously reported studies. Under UV

light irradiation, the semiconductor type metal oxide nanoparticles such as TiO_2 nanoparticles become excited to promote electrons (e_{CB}^-) to the conduction band (CB) from the valence band (VB). This excitation of conduction band electrons (e_{CB}^-) leaves holes (h_{VB}^+) on valance band (VB). This pair of excited electron and hole is commonly known as the exciton. These photogenerated holes (h_{VB}^+) or lack of electrons on the VB can be replenished by the oxidation of organic or inorganic species or by hydroxyl ions (OH^-) in water to produce •OH, Scheme 2.

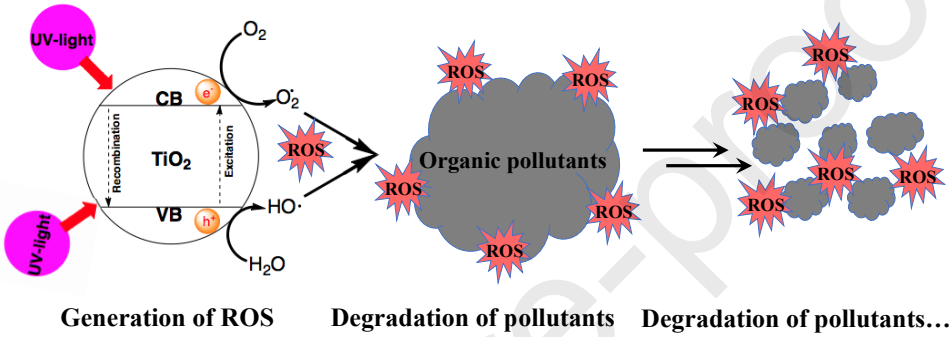

Scheme 2. Photocatalytic generation of ROS followed by the oxidative degradation of organic pollutants.

The excited electrons (e_{CB}^-) on the CB can reduce oxygen (O_2) to oxygen radicals ($•O_2^-$), which in turn can convert into •OH in water. These ROS are very short-lived, highly reactive, and non-selective oxidizing agents that initiate a series of reactions to gradually degrade organic pollutants to mineralization i.e. the production of CO_2 and H_2O.

5. Conclusions

The development of photocatalytic paint consisting of TiO_2 nanoparticles and photopolymer resin is reported. The paint was applied and polymerized/solidified on plastic petri dishes by ultraviolet light irradiation. The painted petri dishes were used for photocatalytic degradation of hazardous organic pollutants *viz.* methyl orange (MO), methylene blue (MB) and indole in water. The sunlight-assisted photocatalytic degradation of these pollutants was found to

be faster compared to the UV-B light-assisted ones. Under UV-B light irradiation, about 80 % MB could be degraded after 120 min, whereas under sunlight irradiation it took about 60 min to degrade 90 % of MB from the same solution. It was confirmed that the polymer embedded TiO_2 nanoparticles generated •OH under the UV-B and sunlight irradiation, which caused the oxidative degradation of the pollutants in water. The results of this study indicate that the photocatalytic paint, developed in this study, could potentially be applied for the degradation of various organic pollutants in water. The paint could also be useful for the preparation of self-disinfecting surfaces and for the degradation of volatile organic pollutants (VOCs and NOx) in the air.

Acknowledgements

Financial support from the National Science Foundation (NSF) grants ERC Nanotechnology-Enabled Water Treatment Center 1449500, CHE-0748913, DMR PREM-1205302, and USDA 2014-38422-22078 are gratefully acknowledged. M.O.M. would like to acknowledge the Welch Foundation Chemistry Department Research Grant (AW-0013).

Author Information

Corresponding Author:

Juan C. Noveron, Email: jcnoveron@utep.edu

Md Tariqul Islam, Email: islam_m@utpb.edu and tariqul.lab@gmail.com

Notes

Authors declare no conflicting financial interest.

Graphical Abstract

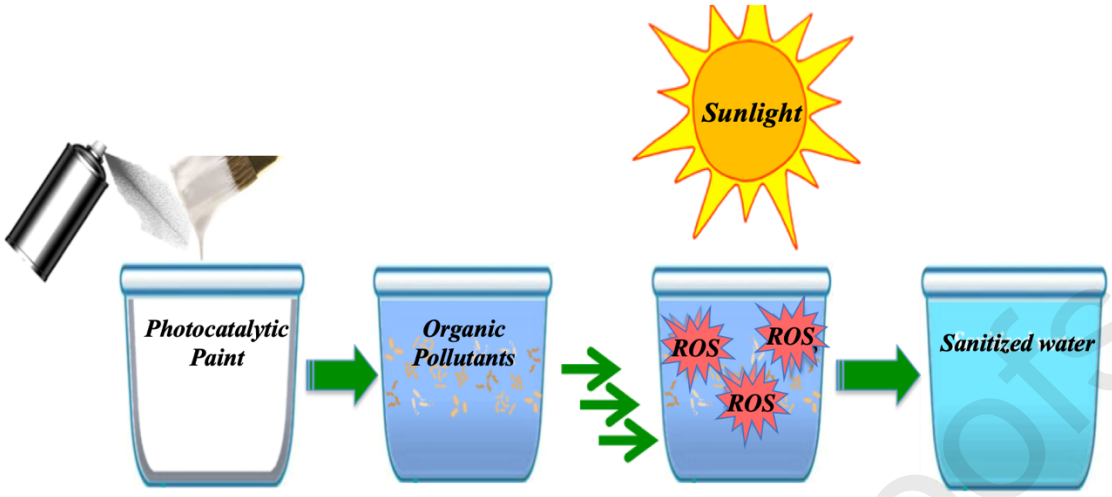

Development of photocatalytic paint based on TiO_2 nanoparticles and photopolymer resin for the degradation of organic pollutants in water under ultraviolet and sunlight irradiation.

References:

[1] Bagheri, S., TermehYousefi, A., & Do, T. O. (2017). Photocatalytic pathway toward degradation of environmental pharmaceutical pollutants: structure, kinetics and mechanism approach. *Catalysis Science & Technology*, *7*(20), 4548-4569.

[2] Chong, M. N., Jin, B., Chow, C. W., & Saint, C. (2010). Recent developments in photocatalytic water treatment technology: a review. *Water research*, *44*(10), 2997-3027.

[3] Kim, S. B., & Hong, S. C. (2002). Kinetic study for photocatalytic degradation of volatile organic compounds in air using thin film TiO2 photocatalyst. *Applied Catalysis B: Environmental*, *35*(4), 305-315.

[4] J. Kiwi, C. Pulgarin, in: W. Daoud (Ed.), Self-cleaning Materials and Surfaces, Woodhead Pub. Co., UK, 2013, pp. 205–224 (Chapter 7).

[5] Bozzi, A., Yuranova, T., Guasaquillo, I., Laub, D., & Kiwi, J. (2005). Self-cleaning of modified cotton textiles by TiO2 at low temperatures under daylight irradiation. *Journal of Photochemistry and Photobiology A: Chemistry*, *174*(2), 156-164.

[6] L. Armelao, D. Barreca, G. Bottaro, A. Gasparotto, C. Maccato, C. Maragno, E. Tondello, U.L. Štangar, M. Bergant, D. Mahne, Photocatalytic and antibacterial activity of TiO2 and Au/TiO2 nanosystems, Nanotechnology 18 (2007) 375709.

[7]O. Carp, C.L. Huisman, A. Reller, Photoinduced reactivity of titanium dioxide, Prog. Solid State Chem. 32 (2004) 33–177.

[8] Li, Z., Fang, Y., Zhan, X., & Xu, S. (2013). Facile preparation of squarylium dye sensitized TiO2 nanoparticles and their enhanced visible-light photocatalytic activity. *Journal of Alloys and Compounds*, *564*, 138-142.

[9] Islam, M. T., Jing, H., Yang, T., Zubia, E., Goos, A. G., Bernal, R. A., ... & Noveron, J. C. (2018). Fullerene stabilized gold nanoparticles supported on titanium dioxide for enhanced photocatalytic degradation of methyl orange and catalytic reduction of 4-nitrophenol. *Journal of environmental chemical engineering*, *6*(4), 3827-3836.

[10] Alvarez, P. J., Chan, C. K., Elimelech, M., Halas, N. J., & Villagrán, D. (2018). Emerging opportunities for nanotechnology to enhance water security. *Nature nanotechnology*, *13*(8), 634.

[11] Bonnefond, A., González, E., Asua, J., Leiza, J., Ieva, E., Brinati, G., ... & Pulgarin, C. (2016). Stable photocatalytic paints prepared from hybrid core-shell fluorinated/acrylic/TiO2 waterborne dispersions. *Crystals*, *6*(10), 136.

[12] Bonnefond, A., González, E., Asua, J. M., Leiza, J. R., Kiwi, J., Pulgarin, C., & Rtimi, S. (2015). New evidence for hybrid acrylic/TiO2 films inducing bacterial inactivation under low intensity simulated sunlight. *Colloids and Surfaces B: Biointerfaces*, *135*, 1-7.

[13] Nakata, K., & Fujishima, A. (2012). TiO2 photocatalysis: Design and applications. *Journal of photochemistry and photobiology C: Photochemistry Reviews*, *13*(3), 169-189.

[14] Stylidi, M., Kondarides, D. I., & Verykios, X. E. (2003). Pathways of solar light-induced photocatalytic degradation of azo dyes in aqueous TiO2 suspensions. *Applied Catalysis B: Environmental*, *40*(4), 271-286.

[15] Tugaoen, H. O. N., Garcia-Segura, S., Hristovski, K., & Westerhoff, P. (2018). Compact light-emitting diode optical fiber immobilized TiO2 reactor for photocatalytic water treatment. *Science of the Total Environment*, *613*, 1331-1338.

[16] Lee, C. G., Javed, H., Zhang, D., Kim, J. H., Westerhoff, P., Li, Q., & Alvarez, P. J. (2018). Porous electrospun fibers embedding TiO2 for adsorption and photocatalytic degradation of water pollutants. *Environmental science & technology*, *52*(7), 4285-4293.

[17] Szczepanik, B. (2017). Photocatalytic degradation of organic contaminants over clay-TiO2 nanocomposites: A review. *Applied Clay Science*, *141*, 227-239.

[18] Ho, C. C., Kang, F., Chang, G. M., You, S. J., & Wang, Y. F. (2019). Application of recycled lanthanum-doped TiO2 immobilized on commercial air filter for visible-light photocatalytic degradation of acetone and NO. *Applied Surface Science*, *465*, 31-40.

[19] Dong, Y., Tang, D., & Li, C. (2014). Photocatalytic oxidation of methyl orange in water phase by immobilized TiO2-carbon nanotube nanocomposite photocatalyst. *Applied Surface Science*, *296*, 1-7.

[20] Monteiro, R. A., Lopes, F. V., Silva, A. M., Ângelo, J., Silva, G. V., Mendes, A. M., ... & Vilar, V. J. (2014). Are TiO_2-based exterior paints useful catalysts for gas-phase photooxidation processes? A case study on n-decane abatement for air detoxification. *Applied Catalysis B: Environmental*, *147*, 988-999.

[21] Delnavaz, M., Ayati, B., Ganjidoust, H., & Sanjabi, S. (2015). Application of concrete surfaces as novel substrate for immobilization of TiO_2 nano powder in photocatalytic treatment of phenolic water. *Journal of Environmental Health Science and Engineering*, *13*(1), 58.

[22] Teixeira, S., Martins, P. M., Lanceros-Méndez, S., Kühn, K., & Cuniberti, G. (2016). Reusability of photocatalytic TiO2 and ZnO nanoparticles immobilized in poly (vinylidene difluoride)-co-trifluoroethylene. *Applied Surface Science*, *384*, 497-504.

[23] Zhang, H., & Zhu, H. (2012). Preparation of Fe-doped TiO2 nanoparticles immobilized on polyamide fabric. *Applied Surface Science*, *258*(24), 10034-10041.

[24] Guo, M. Z., Maury-Ramirez, A., & Poon, C. S. (2016). Self-cleaning ability of titanium dioxide clear paint coated architectural mortar and its potential in field application. *Journal of cleaner production*, *112*, 3583-3588.

[25] Enea, D., Bellardita, M., Scalisi, P., Alaimo, G., & Palmisano, L. (2019). Effects of weathering on the performance of self-cleaning photocatalytic paints. *Cement and Concrete Composites*, *96*, 77-86.

[26] Zeng, J., Liu, S., Cai, J., & Zhang, L. (2010). TiO_2 immobilized in cellulose matrix for photocatalytic degradation of phenol under weak UV light irradiation. *The Journal of Physical Chemistry C*, *114*(17), 7806-7811.

[27] Behpour, M., Mehrzad, M., & Hosseinpour-Mashkani, S. M. (2015). TiO2 thin film: Preparation, characterization, and its photocatalytic degradation of basic yellow 28 dye. *Journal of Nanostructures*, *5*(2), 183-187.

[28] Heshmatpour, F., & Zarrin, S. (2017). A probe into the effect of fixing the titanium dioxide by a conductive polymer and ceramic on the photocatalytic activity for degradation of organic pollutants. *Journal of Photochemistry and Photobiology A: Chemistry*, *346*, 431-443.

[29] Kobayakawa, K., Sato, C., Sato, Y., & Fujishima, A. (1998). Continuous-flow photoreactor packed with titanium dioxide immobilized on large silica gel beads to decompose oxalic acid in excess water. *Journal of Photochemistry and Photobiology A: Chemistry*, *118*(1), 65-69.

[30] Hadjltaief, H. B., Zina, M. B., Galvez, M. E., & Da Costa, P. (2016). Photocatalytic degradation of methyl green dye in aqueous solution over natural clay-supported ZnO–TiO2 catalysts. *Journal of Photochemistry and Photobiology A: Chemistry*, *315*, 25-33.

[31] Alamelu, K., Raja, V., Shiamala, L., & Ali, B. J. (2018). Biphasic TiO2 nanoparticles decorated graphene nanosheets for visible light driven photocatalytic degradation of organic dyes. *Applied Surface Science*, *430*, 145-154.

[32] Dong, Y., Tang, D., & Li, C. (2014). Photocatalytic oxidation of methyl orange in water phase by immobilized TiO2-carbon nanotube nanocomposite photocatalyst. *Applied Surface Science*, *296*, 1-7.

[33] Zhang, D., Lee, C., Javed, H., Yu, P., Kim, J. H., & Alvarez, P. J. (2018). Easily Recoverable, Micrometer-Sized TiO2 Hierarchical Spheres Decorated with Cyclodextrin for Enhanced Photocatalytic Degradation of Organic Micropollutants. *Environmental science & technology*, *52*(21), 12402-12411.

[34] Bilal, M., Rasheed, T., Nabeel, F., Iqbal, H. M., & Zhao, Y. (2019). Hazardous contaminants in the environment and their laccase-assisted degradation–A review. *Journal of environmental management*, *234*, 253-264.

[35] Islam, M. T., Dominguez, N., Ahsan, M. A., Dominguez-Cisneros, H., Zuniga, P., Alvarez, P. J., & Noveron, J. C. (2017). Sodium rhodizonate induced formation of gold nanoparticles supported on cellulose fibers for catalytic reduction of 4-nitrophenol and organic dyes. *Journal of environmental chemical engineering*, *5*(5), 4185-4193.

[36] Islam, M. T., Hernandez, C., Ahsan, M. A., Pardo, A., Wang, H., & Noveron, J. C. (2017). Sulfonated resorcinol-formaldehyde microspheres as high-capacity regenerable adsorbent for the removal of organic dyes from water. *Journal of environmental chemical engineering*, *5*(5), 5270-5279.

[37] Zhu, Y., Fu, Y., & Ni, Q. Q. (2011). Preparation and performance of photocatalytic TiO2 immobilized on palladium-doped carbon fibers. *Applied Surface Science*, *257*(6), 2275-2280.

[38] Duan, Y., Zhang, M., Wang, L., Wang, F., Yang, L., Li, X., & Wang, C. (2017). Plasmonic Ag-TiO2− x nanocomposites for the photocatalytic removal of NO under visible light with high selectivity: The role of oxygen vacancies. *Applied Catalysis B: Environmental*, *204*, 67-77.

[39] Nawi, M. A., & Zain, S. M. (2012). Enhancing the surface properties of the immobilized Degussa P-25 TiO2 for the efficient photocatalytic removal of methylene blue from aqueous solution. *Applied Surface Science*, *258*(16), 6148-6157.

[40] Cantini, M., Rico, P., Moratal, D., & Salmerón-Sánchez, M. (2012). Controlled wettability, same chemistry: biological activity of plasma-polymerized coatings. *Soft Matter*, *8*(20), 5575-5584.

[41] Islam, M. T., Rosales, J., Ricardo, S. A., Ghadimi, S., & Noveron, J. (2019). Rapid Synthesis of Ultrasmall Platinum Nanoparticles Supported on Macroporous Cellulose Fibers for Catalysis. *Nanoscale Advances*, 1, 2953-2964.

[42] Erdem, B., Hunsicker, R. A., Simmons, G. W., Sudol, E. D., Dimonie, V. L., & El-Aasser, M. S. (2001). XPS and FTIR surface characterization of TiO2 particles used in polymer encapsulation. *Langmuir*, *17*(9), 2664-2669.

[43] Islam, M. T., Hernandez, C., Ahsan, M. A., Pardo, A., Wang, H., & Noveron, J. C. (2017). Sulfonated resorcinol-formaldehyde microspheres as high-capacity regenerable adsorbent for the

removal of organic dyes from water. *Journal of environmental chemical engineering*, *5*(5), 5270-5279.

[44] Islam, M. T., Saenz-Arana, R., Hernandez, C., Guinto, T., Ahsan, M. A., Bragg, D. T., ... & Noveron, J. C. (2018). Conversion of waste tire rubber into a high-capacity adsorbent for the removal of methylene blue, methyl orange, and tetracycline from water. *Journal of Environmental Chemical Engineering*, *6*(2), 3070-3082.

[45] Islam, M. T., Hyder, A. G., Saenz-Arana, R., Hernandez, C., Guinto, T., Ahsan, M. A., ... & Noveron, J. C. (2019). Removal of methylene blue and tetracycline from water using peanut shell derived adsorbent prepared by sulfuric acid reflux. *Journal of Environmental Chemical Engineering*, *7*(1), 102816.

[46] Islam, M. T., Saenz-Arana, R., Hernandez, C., Guinto, T., Ahsan, M. A., Kim, H., ... & Noveron, J. C. (2018). Adsorption of methylene blue and tetracycline onto biomass-based material prepared by sulfuric acid reflux. *RSC advances*, *8*(57), 32545-32557.

[47] Rtimi, S., Robyr, M., Pulgarin, C., Lavanchy, J. C., & Kiwi, J. (2016). A new perspective in the use of FeOx-TiO2 photocatalytic films: Indole degradation in the absence of Fe-leaching. *Journal of catalysis*, *342*, 184-192.

[48] Islam, M. T., Dominguez, A., Alvarado-Tenorio, B., Bernal, R. A., Montes, M. O., & Noveron, J. C. (2019). Sucrose-Mediated Fast Synthesis of Zinc Oxide Nanoparticles for the Photocatalytic Degradation of Organic Pollutants in Water. *ACS Omega*, *4*(4), 6560-6572.

[49] K. Ishibashi, A. Fujishima, T. Watanabe and K. Hashimoto, Electrochem. Commun., 2000, 2, 207–210